Chapter 6

Fatigue crack growth rate behavior of Al-Mg-Zn alloy under 3.5 % NaCl environment

6.1 Introduction

In this chapter we investigated the fatigue crack growth rate (FCGR) of Al-Mg-Zn alloy under five different conditions: solution heat treated (SHT), SHT +peak aged (PA), SHT +45% cold rolled (CR), SHT +60% warm rolled (WR), and SHT +PA +90% CR, in a 3.5% NaCl solution and compared it to the normal condition. Electrochemical testing was performed using a Gamry Interface 1010E electrochemical workstation. Microstructural characterization was carried out using scanning electron microscopy (SEM). Mechanical properties were evaluated through fatigue crack growth rate testing. The three regions of fatigue pre crack((i) crack initiation, (ii) crack propagation, (iii) unstable crack growth, are investigated very well with the help of Paris law and fractography of the pre-cracked samples. Results shows that the threshold stress intensity factor range (ΔK) is reduced for all five conditions samples, and the fatigue crack growth rate increases across the entire ΔK regime compared to normal condition due earlier formation of persisting slip bands (PSBs) because of corrosion effect. In stable crack growth region length of striations as well as gap between them also increased which showing poor fatigue life.

6.2 Fatigue crack growth rate behavior

The da/dN vs ΔK curve is a fundamental plot used in fatigue crack growth (FCG) analysis to describe how a crack grows in a material under cyclic loading. It shows the relationship between:

da/dN: the crack growth rate per load cycle (typically in mm/cycle or m/cycle), and

ΔK: the stress intensity factor range (in MPa√m), representing the severity of the cyclic loading at the crack tip. Fig. 6.1 showing the da/dN vs ΔK curve for both normal and 3.5% NaCl condition for all five conditions samples (SHT +peak aged (PA), SHT +45% cold rolled (CR), SHT +60% warm rolled (WR), and SHT +PA +90% CR). In which red color graph is for 3.5% NaCl condition and blue color graph is for normal condition. The normal condition graph is taken from the Fig. 4.12 of chapter 4[148]. Fig. (a), (b), (c), (d) and (e) are the Paris law curve for SHT, SHT+PA, SHT+45% CR, SHT+60% WR and SHt+PA+90% CR samples respectively. In which the region I, II and III is differentiated on the basis of the slope of the curve. The threshold value for all five conditions sample in normal and in 3.5 % NaCl solution is described in Table 6.1. fatigue life is calculated with the help of equation 4.3 of chapter 4 and demonstrated in Table 6.2

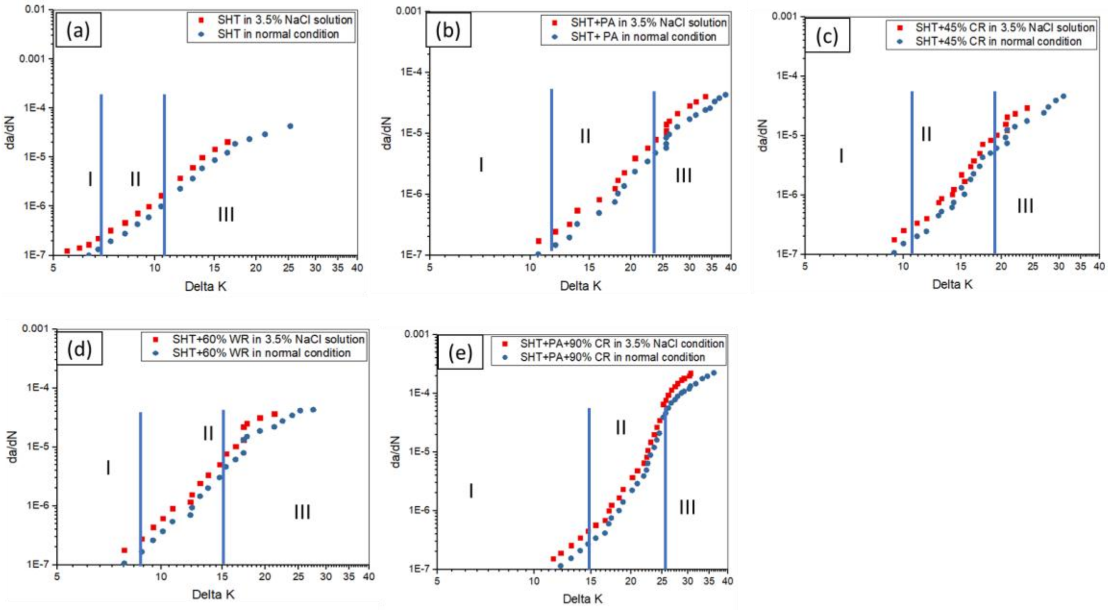

Fig. 6.1 Paris law curve for all five conditions sample (SHT+ peak aged (PA), SHT+45% cold rolled (CR), SHT+60% warm rolled (WR) and SHT+PA+90% CR)

Table 6.1: Threshold value for SHT+ peak aged (PA), SHT+45% cold rolled (CR), SHT+60% warm rolled (WR) and SHT+PA+90% CR samples in normal and 3.5% NaCl solution.

Conditions	**ΔK value for normal condition (MPa√m)**[148]	**ΔK value for 3.5% NaCl solution condition (MPa√m)**
SHT	5.9	5.3
SHT+PA	10	9.8
SHT+45% CR	9	8.7
SHT+60% WR	7.9	7.1
SHT+PA+90% CR	12	11.5

Table 6.2: No. of cycles for all five conditions in 3.5 % NaCl solution with as received condition.

Conditions	SHT	SHT+PA	SHT+45% CR	SHT+60%WR	SHT+PA+90% CR	As received
No. of cycles (N)	100020	234320	115220	125321	283261	340000
C	6.849× 6	8.654×10^{-11}	5.329×10^{-10}	9.217×10^{-8}	7.534×10^{-12}	4.3316×10^{-9}
M	7.652	2.761	3.537	5.578	2.135	1.912

6.3 Fractography

6.3.1 Fractography of fatigue pre crack region for SHT sample in normal and 3.5% NaCl

Fig. 6.2 (a) is illustrating the fatigue pre crack region of SHT sample in normal condition while Fig. 6.2(b) displays the same region for the SHT sample exposed to 3.5% NaCl solution. In the corrosive environment, both the crack initiation and propagation regions are smaller compared to the normal condition, indicating that crack initiation occurs earlier and crack propagation is significantly faster in 3.5% NaCl. Upon comparing the stable crack growth regions in Figure 6.2(c) (normal condition) and Fig. 6.2(d) (3.5% NaCl solution), it is observed that the striation length increases in the presence of the NaCl solution. Furthermore, the spacing between striations becomes so large that it essentially transitions into a continuous crack as shown in Fig. 6.2(d). Corrosion products are observed in the unstable crack growth region, indicating that corrosion has affected the sample not only externally but also internally.

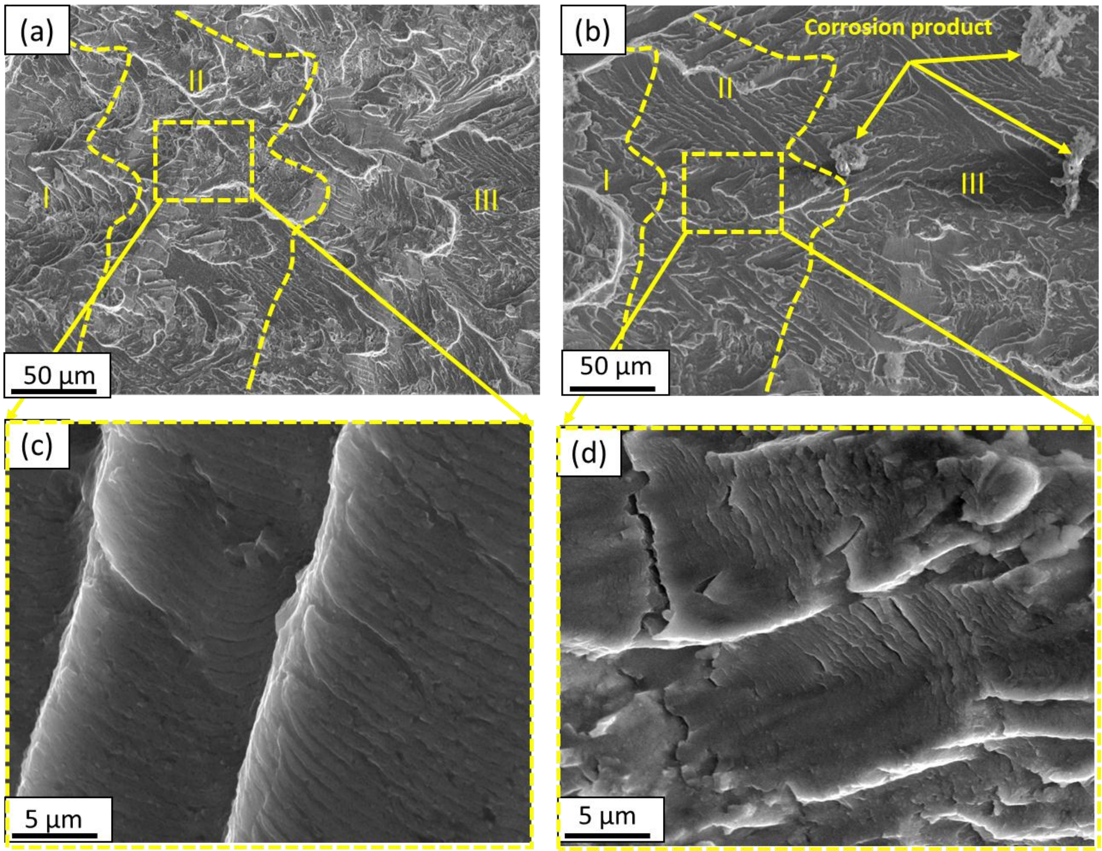

Fig. 6.2 Fractography image of fatigue pre crack region for SHT sample(a) normal condition, (b) 3.5% NaCl solution, (c, d) fractography image of stable crack growth region of SHT sample in normal and 3.5% NaCl solution

6.3.2 Fractography of fatigue pre crack region for SHT+PA sample in normal and 3.5% NaCl

Fig. 6.3(a) illustrates the fatigue pre-crack region of the SHT+PA sample under normal conditions, whereas Fig. 6.3(b) shows the corresponding region in a 3.5% NaCl solution. In the NaCl environment, both the crack initiation and propagation regions are smaller compared to the normal condition, indicating that crack initiation occurs earlier and crack propagation proceeds more rapidly in the corrosive medium. A comparison of the stable crack growth region in normal conditions **(**Fig. 6.3(c)**)** and in 3.5% NaCl solution **(**Fig. 6.3(d)**)** reveals that the striation length increases significantly in the saline environment. Additionally, the spacing between striations becomes large. Corrosion product is also observed in the stable crack growth region, indicating that corrosion has affected this sample not only externally but also internally, which is detrimental to its structural integrity.

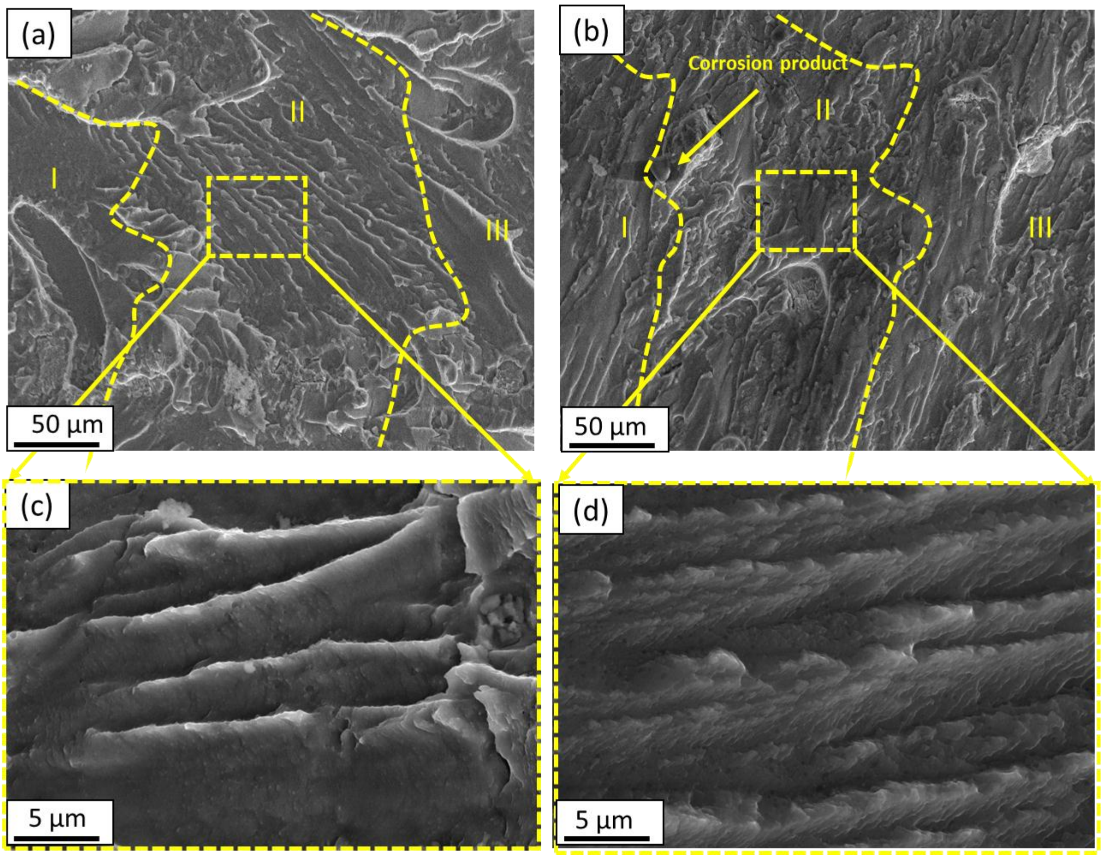

Fig. 6.3 Fractography image of fatigue pre crack region for SHT+PA sample(a) normal condition, (b) 3.5% NaCl solution, (c, d) fractography image of stable crack growth region of SHT+PA sample in normal and 3.5% NaCl solution

6.3.3 Fractography of fatigue pre crack region for SHT+45% CR sample in normal and 3.5% NaCl

Fig. 6.4(a) presents the fatigue pre-crack region of the SHT+45% CR sample under ambient (non-corrosive) conditions, while Fig. 6.4(b) depicts the corresponding region after exposure to a 3.5% NaCl solution. In the saline environment, both the crack initiation and propagation zones are notably reduced in size compared to those observed under normal conditions. This suggests that crack initiation occurs earlier and propagation progresses more rapidly in the presence of a corrosive medium. A comparison of the stable crack growth regions under normal conditions (Figure 6.4(c) and in the 3.5% NaCl environment (Figure 6.3(d)) reveals a significant increase in striation length within the corrosive medium. Furthermore, the spacing between striations is markedly wider. The presence of corrosion products in the stable crack growth region further indicates that corrosion has affected the sample not only on the surface but also internally, thereby compromising its structural integrity also.

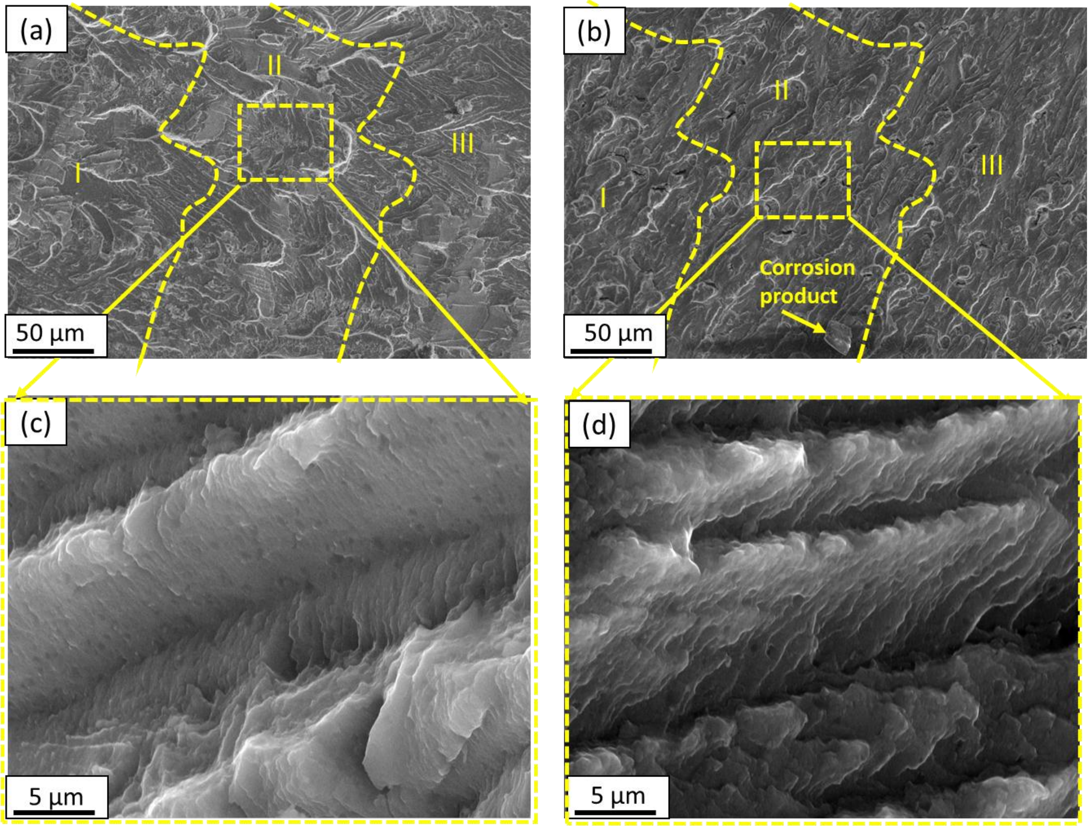

Fig. 6.4 Fractography image of fatigue pre crack region for SHT+45% CR sample(a) normal condition, (b) 3.5% NaCl solution, (c, d) fractography image of stable crack growth region of SHT+45% CR sample in normal and 3.5% NaCl solution

6.3.4 Fractography of fatigue pre crack region for SHT+60% WR sample in normal and 3.5% NaCl

Fig. 6.5(a) presents the fractography of the pre-crack region of the SHT + 60% WR sample under normal conditions, while Fig. 6.5(b) shows the corresponding region for the same sample exposed to a 3.5% NaCl solution. A comparison of Figs. 6.5(a) and 6.5(b) reveals that both the crack initiation and stable crack growth regions are reduced in the presence of the 3.5% NaCl environment. Further, Figs. 6.5(c) and 6.5(d) illustrate the stable crack growth regions under normal and corrosive conditions, respectively. Under normal conditions, the striations are shorter and closely spaced, whereas in the 3.5% NaCl solution, the striations are longer and more widely spaced eventually merging into a continuous crack path.

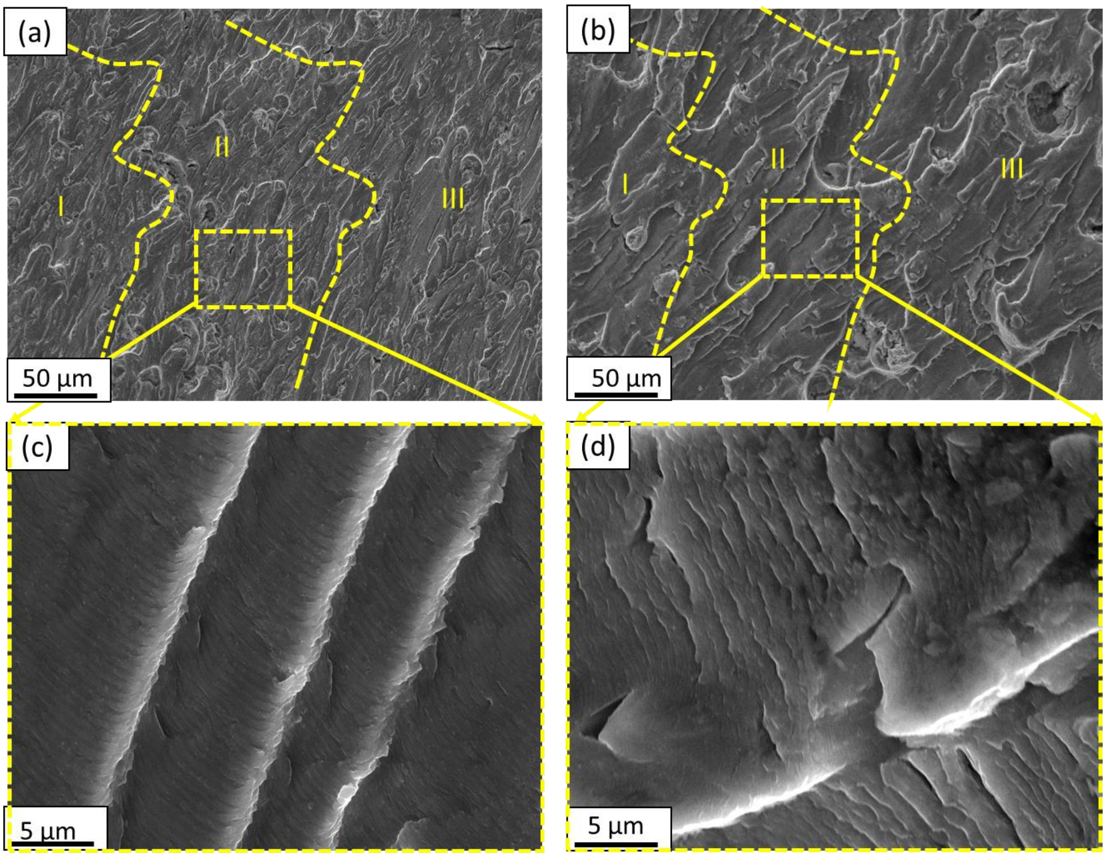

Fig. 6.5 Fractography image of fatigue pre crack region for SHT+60% WR sample(a) normal condition, (b) 3.5% NaCl solution, (c, d) fractography image of stable crack growth region of SHT+60% WR sample in normal and 3.5% NaCl solution

6.3.5 Fractography of fatigue pre crack region for SHT+PA+90% CR sample in normal and 3.5% NaCl

Fig. 6.6(a) presents the fractographic image of the pre-crack region of the SHT+PA+90% CR sample under normal conditions, while Fig. 6.6(b) shows the corresponding region after exposure to a 3.5% NaCl solution. A comparison of Figs. 6.5(a) and 6.5(b) reveals that both the crack initiation and stable crack growth regions are reduced in size in the corrosive environment. Furthermore, Figs. 6.6(c) and 6.6(d), which depict the stable crack growth regions under normal and corrosive conditions respectively, indicate that the striations are shorter and more closely spaced under normal conditions. In contrast, in the 3.5% NaCl solution, the striations are longer, more widely spaced.

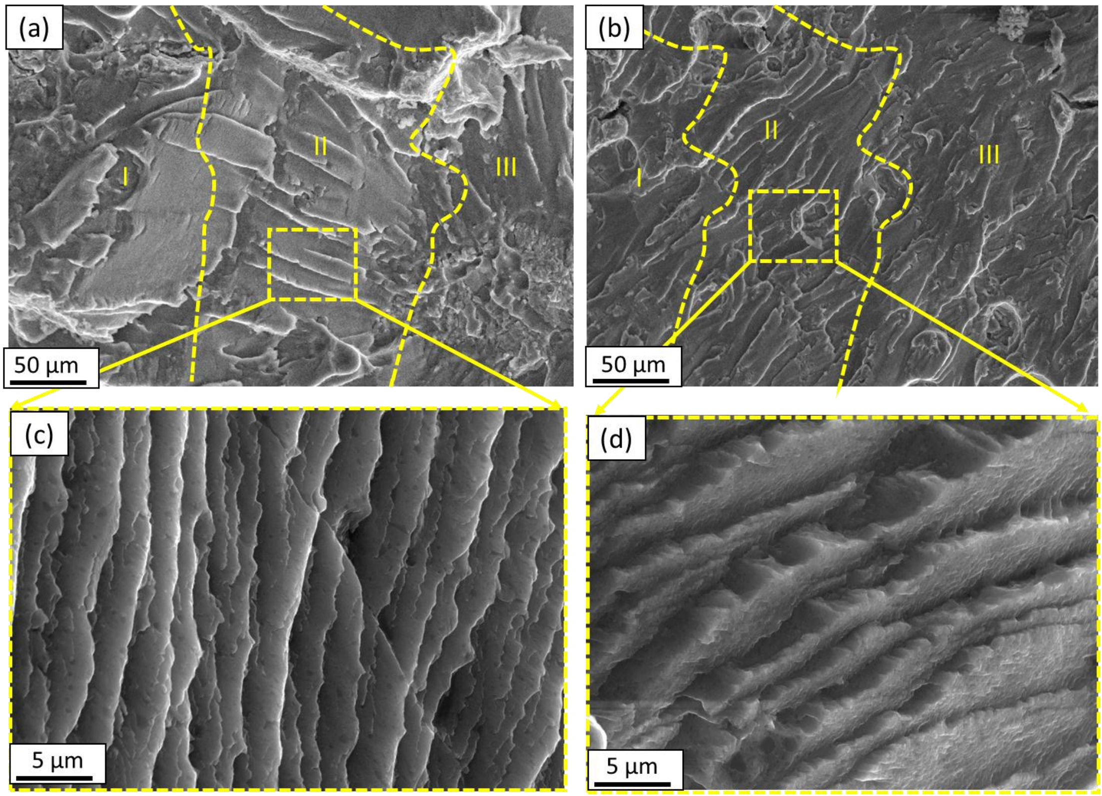

Fig. 6.6 Fractography image of fatigue pre crack region for SHT+PA+90% sample(a) normal condition, (b) 3.5% NaCl solution, (c, d) fractography image of stable crack growth region of SHT+PA+90% sample in normal and 3.5% NaCl solution

6.4 Discussion

6.4.1 Effect of 3.5% NaCl solution of all three regions of Paris curve

The fatigue crack growth rate (FCGR) behavior of the 7075 Al alloy in a 3.5% NaCl environment demonstrates significant degradation in fatigue resistance due to the combined effects of cyclic loading and corrosion[73,75].

Region I: (Threshold Region) In Region I, crack initiation occurs at a lower ΔK threshold (Fig. 6.1) due to corrosion pits or intergranular attack which may serve as crack initiation sites[168]. Chloride ions penetrate crack tips and interfere with crack closure mechanisms, lowering the effective ΔK value[169]. The aggressive chloride ions in the NaCl solution accelerate crack initiation by attacking the passive oxide film on the alloy surface[170], leading to localized corrosion and stress concentration[146,171]. As a result, the threshold stress intensity factor range (ΔK) is reduced,[172] and the fatigue crack growth rate increases across the entire ΔK regime compared to normal condition[173].

Region II: Paris Regime (Linear Log-Log or stable crack growth region) In this region, crack growth follows the Paris law which is described by the equation 4.2 of chapter 4[148]. In the Paris regime, the slope of the log(da/dN) vs. log(ΔK) curve and (Paris exponent, n) tends to be steeper (Fig. 6.1) in the NaCl environment, indicating increased sensitivity of crack growth to stress intensity range[23]. This behavior can be attributed to synergistic interactions between mechanical fatigue damage and electrochemical attack at the crack tip[174]. The corrosion products generated inside the crack may act as wedges that promote crack opening and reduce crack closure effects, enhancing crack propagation[74,175].

Region III: (Rapid Crack Growth or unstable crack growth region)

At high ΔK, near the material's fracture toughness K the crack growth rate accelerates dramatically. Crack growth becomes unstable, leading to sudden failure[43,145]. In Region III, the alloy exhibits unstable crack growth[139], and fracture occurs at lower critical stress intensity values (Kc) than in normal condition due to corrosion-induced embrittlement.

6.4.2 effect of 3.5% NaCl solution on persisting slip bands (PSBs) formation

Corrosive environments (e.g., NaCl) facilitate anodic dissolution at the surface. This reduces local yield strength, easing dislocation movement and promoting earlier formation of PSBs[176]. Chloride ions break down passive oxide films which promotes localized corrosion (e.g., pitting). These pits act as stress concentrators, enhancing slip localization and accelerating PSB formation at pit roots[59]. In corrosive environments, hydrogen may be generated and absorbed by the metal. Hydrogen enhances localized plasticity[177,178], increasing dislocation mobility and contributing to unstable PSB growth. It also reduces cohesive strength, promoting intergranular decohesion near PSBs[179]. Corrosion-assisted slip band formation is more intense than in normal condition. Crack nucleation occurs earlier due to the combined effect of mechanical strain and chemical attack[54].

6.4.3 Effect of 3.5% NaCl solution on striation length

Corrosive species (like Cl^- in NaCl solution) penetrate the crack tip, weakening the material and promoting faster crack advance per cycle[60,180]. Striations appear wider and longer (Figs.6.2 (d), 6.3 (d), 6.4(d), 6.5(d), 6.6(d)) because each fatigue cycle causes a greater crack advance due to combined mechanical and chemical effects[181]. In normal condition, oxide debris or roughness can induce crack closure[182], slowing down crack growth with shorter striation (Figs.6.2 (c), 6.3 (c), 6.4(c), 6.5(c), 6.6(c)). In a corrosive medium, oxide formation may be prevented or altered, reducing crack closure and thus increasing effective stress intensity, which increases striation length[183,184]. Corrosion can blur or obscure the striation pattern due to intergranular attack**,** pitting, or corrosion product formation, especially at lower stress intensity ranges[185,186]. This makes striation length measurement more challenging and less reliable[187,188]. In 7075 Al alloy, corrosion can induce hydrogen embrittlement that is produce hydrogen atoms[178,189], which diffuse into the metal and reduce its ductility[190,191]. This facilitates easier crack opening and extension, again increasing striation spacing[88,180]. This might result in fewer visible striations and more brittle features[171] (cleavage or intergranular fractures) as shown in Figs. 6.2(d) and 6.5(d) changing the fracture surface morphology. In corrosive environments, crack propagation is faster due to chemical attack at the crack tip. This leads to greater material removal per fatigue cycle, resulting in longer striations[192].